Translational Oncology 26 (2022) 101536

Contents lists available at ScienceDirect

Translational Oncology

journal homepage: www.elsevier.com/locate/tranon

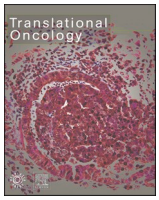

Original Research

CT radiomics combined with clinical variables for predicting the overall survival of hepatocellular carcinoma patients after hepatectomy

Ying Liu [a,#], Xiaoqin Wei [a,#], Xinrui Zhang [a], Caifeng Pang [a], Mingkai Xia [a], Yong Du [b,*]

[a] School of Medical Imaging, North Sichuan Medical College, Nanchong City 637000, Sichuan Province, China
[b] Department of Radiology, the Affiliated Hospital of North Sichuan Medical College, Nanchong City 637000, Sichuan Province, China

ARTICLE INFO

Keywords:
Radiomics
Hepatocellular carcinoma
Hepatectomy
Prognosis

ABSTRACT

Purpose: To establish a model for assessing the overall survival (OS) of the hepatocellular carcinoma (HCC) patients after hepatectomy based on the clinical and radiomics features.
Methods: This study recruited a total of 267 patients with HCC, which were randomly divided into the training (N = 188) and validation (N = 79) cohorts. In the training cohort, radiomic features were selected with the intra-reader and inter-reader correlation coefficient (ICC), Spearman's correlation coefficient, and the least absolute shrinkage and selection operator (LASSO). The radiomics signatures were built by COX regression analysis and compared the predictive potential in the different phases (arterial, portal, and double-phase) and regions of interest (tumor, peritumor 3 mm, peritumor 5 mm). A clinical-radiomics model (CR model) was established by combining the radiomics signatures and clinical risk factors. The validation cohort was used to validate the proposed models.
Results: A total of 267 patients 86 (45.74%) and 37 (46.84%) patients died in the training and validation cohorts, respectively. Among all the radiomics signatures, those based on the tumor and peritumor (5 mm) (AP-TP5-Signature) showed the best prognostic potential (training cohort 1–3 years AUC:0.774–0.837; validation cohort 1–3 years AUC:0.754–0.810). The CR model showed better discrimination, calibration, and clinical applicability as compared to the clinical model and radiomics features. In addition, the CR model could perform risk-stratification and also allowed for significant discrimination between the Kaplan-Meier curves in most of the subgroups.
Conclusions: The CR model could predict the OS of the HCC patients after hepatectomy.

Introduction

Hepatocellular carcinoma (HCC) is the most common pathological type of Primary hepatic carcinoma (PHC) [1], which accounts for approximately 75%−85% of the PHC [2]. The Barcelona clinical liver cancer (BCLC) [3], the most widely used liver cancer staging system, classifies patients into five stages and recommends treatment for each stage by assessing their tumor burden, liver function and health status. Although the BCLC guidelines have recommended hepatectomy for the HCC patients with a single tumor [3], recent studies showed that hepatectomy could also prolong the survival of some HCC patients with intermediate or advanced stages [4–9]. Due to the heterogeneity of HCC patients [10], not all patients benefit from hepatectomy. The prognosis of patients might be closely related to the clinical factors, laboratory variables, and internal lesion features. Therefore, a model is needed, which can predict the prognosis of HCC patients after hepatectomy.

Different studies have extensively used radiomics in a variety of medical disciplines and have obtained a huge number of positive outcomes. This has been made possible by the rapid advancement of imaging and computing technologies. [11]. Radiomics is the process of obtaining the quantitative aspects of medical images using computer-based algorithms. These quantitative features are then utilized in the construction of models for diagnosing, grading, staging, or predicting the effectiveness of treatments [12]. Numerous studies showed that the radiomics features correlated with the biological characteristics of tumors and provided predictive information, which was far beyond the clinical features [13]. Radiomics showed a high predictive capability for the staging, differential diagnosis, prognosis,

* Corresponding author.
E-mail address: duyong@nsmc.edu.cn (Y. Du).
# These authors contributed equally to this article.

https://doi.org/10.1016/j.tranon.2022.101536
Received 28 June 2022; Received in revised form 29 August 2022; Accepted 4 September 2022

and treatment selection of HCC [14,15]. Therefore, it is possible to create models, which can assess the survival of HCC patients after hepatectomy using radiomics.

The values of CT radiomics have been investigated for the prognosis of hepatectomy [16–18]. The radiomics characteristics of the tumor were extracted based on a single-phase (arterial phase or portal phase) or multiphase without considering the tumor microenvironment. In recent years, numerous studies confirmed that the inflammatory state of the tumor microenvironment might affect tumorigenesis and progression [1921] and the peritumor region could provide key information on tumor micro-metastasis and micro-invasion [22]. The risk factors for the patients included microvascular invasion, CD68+ cell density, and epithelial cell adhesion molecule (EpCAM) in the peritumoral tissues [23,24]. These biomarkers were derived from the postoperative tissue samples, which were not only invasive but also raised the possibility that the samples acquired might not be the representative of heterogeneity and burden of all the patients. In contrast, the peritumor radiomics features, which were obtained preoperatively and non-invasively, could predict the prognosis of HCC patients, thereby providing a novel method for the prediction of prognosis. Few studies have predicted the overall survival (OS) of patients after hepatectomy by integrating the tumor and peritumor radiomics characteristics based on multiphase CT.

This study aimed to develop and validate a model for predicting the OS of patients by combining the clinical variables and radiomics features retrieved from the tumor and peritumor regions.

Materials and methods

Population

This study was approved by the Ethical Review Committee of the Affiliated Hospital of North Sichuan Medical College (AHNSMC), which waived the informed consent of the participants.

A total of 661 HCC patients were recruited from June 2016 to July 2021, who underwent hepatectomy procedures at the AHNSMC. Based on the inclusion and exclusion criteria, a total of 267 patients were enrolled in this study, who were randomly divided (at a ratio of 7:3) into the training and validation cohorts. The inclusion criteria were as follows: (1) the patients underwent hepatectomy and were followed-up and (2) the patients were diagnosed with HCC based on the histopathological confirmation. The exclusion criteria were as follows: (1) the patients, who had already received other systemic or local antitumor therapies before hepatectomy; (2) the patients, who did not receive Computed Tomography (CT) or performed CT more than one month before hepatectomy; (3) patients with poor quality CT images would be excluded; and (4) the patients, who had incomplete laboratory examinations, demographic information, and follow-up data.

Follow-up

Following hepatectomy, the patients were followed up. And 3 months (first year postoperative), 6 months (second year postoperative) and 6–12 months (third year onward) were used as follow-up intervals. As a part of the follow-up examinations, the liver function tests, ultrasounds, abdominal CT scans, and other necessary laboratory variables were evaluated in the patients.

The OS rate was calculated at the primary endpoint of the study, which was defined as the time duration between hepatectomy and death of the final date of observation.

CT scan

The scanning parameters are listed in Supplementary Table 1. All the patients received the standard abdominal enhanced CT within one month before surgery. They were injected intravenously with 60 mL of contrast medium at a rate of 3.0–3.5 mL/s using a high-pressure syringe. After 30 and 60 s, the images of the arterial and portal phases were obtained, respectively.

Radiomics signature

Pyradiomics package (https://pyradiomics.readthedocs.io/en/v3.0.1/) was used to normalize the voxel spacing by resampling the images to a voxel size (1 mm × 1 mm × 1 mm) using a linear interpolation approach. By discretizing the values of voxel intensity with a fixed bin width (25HU), the image noise and equalize voxel intensity were controlled [25].

The preprocessed images were then imported into the 3D Slicer software, in which, reader 1 indicated the region of interest (ROI) in each transverse section along the tumor border. The peritumor ROIs

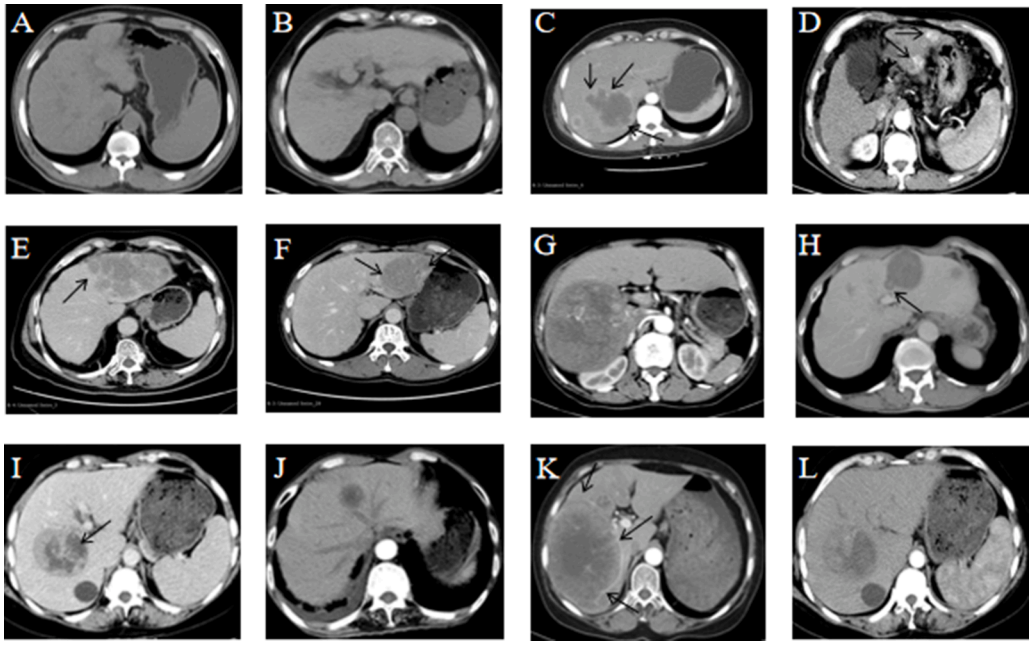

Fig. 1. Definition of the radiological characteristics. The black arrows show the presence of cirrhosis (A); absence of cirrhosis (B); the presence of fusion lesions (C); absence of fusion lesions (D); absence of tumor capsule (E); tumor with unintegral capsule (F); tumor with integral capsule (G); the breakthrough of tumor capsule (H); the presence of intra-tumoral necrosis (I); absence of intra-tumoral necrosis (J); the presence of arterial peritumoral enhancement (K); and absence of arterial peritumoral enhancement (L).

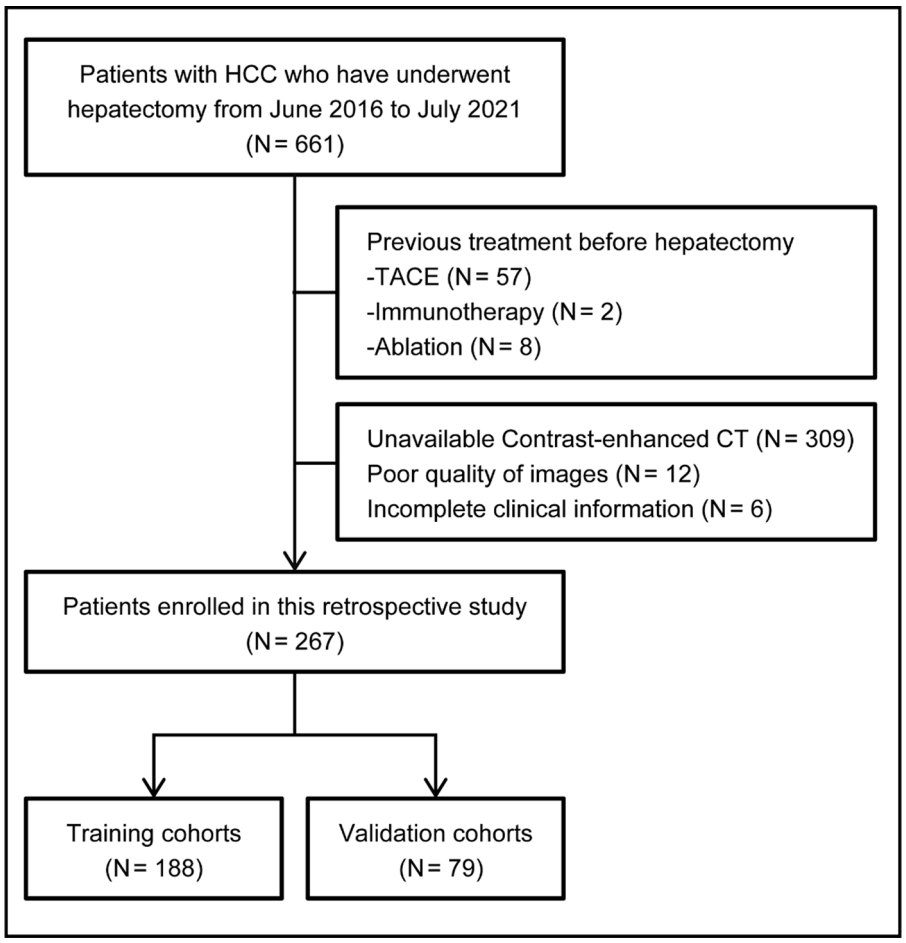

Fig. 2. Include and exclude flowchart. HCC, hepatocellular carcinoma; TACE, transcatheter arterial chemoembolization.

were automatically reconstructed using the erosion and dilation technique, expanding 3 mm and 5 mm outward from the tumor perimeter.

The intra-reader and inter-reader reproducibility were used to test the segmentation's stability. A total of 20 patients were selected randomly, and the ROIs in these patients were independently defined by Reader 1 and Reader 2 to determine inter-reader reproducibility using the intraclass correlation coefficient (ICC). After 1 week, reader 1 again delineated the ROIs of these 20 patients to measure the intra-reader reproducibility.

The radiomics features were extracted using the Pyradiomics package. The retrieved features and their detailed algorithms were available at https://pyradiomics.readthedocs.io/en/latest/features.html.. Before selection, the feature values were normalized using Z-score to remove dimension divergence amongst the radiomics features. In order to limit the risk of overfitting, the features were selected as follows: first, the features with intra-reader and inter-reader ICC <0.70 were removed; second, Spearman's correlation coefficient (hereafter denoted as "R") between the features was measured, and those with $|R| > 0.6$ were excluded; third, the least absolute shrinkage and selection operator (LASSO) regression analysis was used to obtain the reliable prognostic features.

After extracting and selecting the radiomics elements of each phase and their combination, the radiomics signatures were produced and their predictive values were assessed. Then, the radiomics signatures of the peritumor regions (3 mm, 5 mm) were constructed and their prognostic performance was assessed.

Clinical variables and radiological characteristics

A standardized form was created for collecting the clinical variables. The form included the following parameters; age, sex, diabetes, HBV infection, alanine aminotransferase (ALT), serum albumin (ALB), prothrombin time (PT), international normalized ratio (INR), glutamyl transpeptidase (GGT), total bilirubin (TBIL), platelet count (PLT), serum creatinine (sCr), aspartate aminotransferase (AST), albumin-bilirubin (ALBI) grade, Child-Pugh, Eastern Cooperative Oncology Group Performance Status (ECOG-PS), and BCLC stage. For detailed clinical features see Supplementary Text 1. The patient's Alpha-fetoprotein (AFP) data were excluded because some HCC patients were not tested for AFP values (67/267).

The radiological characteristics were independently evaluated by two physicians. The evaluated characteristics included the following: (1) tumor diameter; (2) tumor location (right, left, or across); (3) tumor number; (4) cirrhosis (present or absent); (5) fusion lesions (present or absent); (6) tumor capsule (absent, unintegral, integral, or breakthrough); (7) intra-tumoral necrosis (absent or present); and (8) arterial peritumoral enhancement (absent or present). Fig. 1 presents the definition of radiological characteristics.

In order to analyze the clinical variables and radiological parameters, a univariate Cox proportional hazards regression was performed. The candidate factors related to prognosis were included in the multivariable analysis. The Akaike information criterion employed a backward stepwise selection strategy for the multivariable analysis.

Table 1
Clinical and radiological characteristics of the patients.

Characteristics	Training cohort (N = 188)	Validation cohort (N = 79)	P
Age (years), median (range)	58 (49.0–67.0)	58 (48.5–63.5)	0.51
Sex, No. (%)			
Male	162 (86.2)	66 (83.5)	0.58
Female	26 (13.8)	13 (16.5)	
HBV infection, No. (%)			
Absent	40 (21.3)	20 (25.3)	0.47
Present	148 (78.7)	59 (74.7)	
Diabetes mellitus, No. (%)			
Absent	174 (92.6)	72 (91.1)	0.70
Present	14 (7.4)	7 (8.9)	
Cirrhosis, No. (%)			
Absent	142 (75.5)	60 (75.9)	0.94
Present	46 (24.5)	19 (24.1)	
PLT (109/L), median (range)	132 (95.8–193.0)	142 (104.5–192.0)	0.43
GGT (U/L), median (range)	76 (37.3–156.0)	73 (43.5–173.1)	0.73
ALB (g/L), mean ± SD	39.6 ± 5.6	39.3 ± 5.8	0.62
TBIL (μmol/L), median (range)	16 (12.6–23.2)	16 (12.5–23.8)	0.75
sCr (μmol/L), median (range)	67 (57.1–74.5)	67 (54.6–78.9)	0.66
PT (*sec*), median (range)	13.7 (13.1–14.3)	13.8 (13.0–14.3)	0.92
ALT (U/L), median (range)	39 (24.0–62.0)	31 (21.5–54.3)	0.06
INR, median (range)	1.1 (1.0–1.1)	1.1 (1.0–1.1)	0.59
AST (U/L), median (range)	46 (31.0–71.6)	46 (29.2–64.7)	0.37
Tumor Diameter (mm), median (range)	5.5 (3.8–8.43)	6.0 (3.9–7.8)	0.81
Tumor location, No. (%)			
Left	62 (33.0)	32 (40.5)	0.50
Right	113 (60.1)	42 (53.2)	
Across	13 (6.9)	5 (6.3)	
Tumor number, No. (%)			
1	101 (53.7)	47 (59.5)	0.83
2	42 (22.4)	9 (11.4)	
≥3	45 (23.9)	23 (29.1)	
Fusion lesions, No. (%)			
Absent	102 (54.3)	48 (60.8)	0.33
Present	86 (45.7)	31 (39.2)	
Tumor capsule, No. (%)			
Absent	45 (24.0)	25 (31.6)	0.97
Integral	82 (43.6)	41 (51.9)	
Unintegral	35 (18.6)	10 (12.7)	
Breakthrough	26 (13.8)	3 (3.8)	
Intra-tumoral necrosis, No. (%)			
Absent	68 (36.2)	30 (38.0)	0.78
Present	120 (63.8)	49 (62.0)	
Arterial peritumoral enhancement, No. (%)			
Absent	67 (35.6)	24 (30.4)	0.41
Present	121 (64.4)	55 (69.6)	
ECOG-PS, No. (%)			
0	32 (17.0)	15 (19.0)	0.39
1	150 (79.8)	60 (75.9)	
2	5 (2.7)	4 (5.1)	
3	1 (0.5)	0 (0.0)	
ALBI grade, No. (%)			
Grade 1	91 (48.4)	36 (45.6)	0.09
Grade 2	93 (49.5)	41 (51.9)	
Grade 3	4 (2.1)	2 (2.5)	
Child-Pugh, No. (%)			
Class A	167 (88.8)	70 (88.6)	0.96
Class B	21 (11.2)	9 (11.4)	
BCLC stage, No. (%)			
0 stage	5 (2.6)	1 (1.3)	0.18
A stage	90 (47.9)	39 (49.4)	
B stage	53 (28.2)	20 (25.3)	
C stage	40 (21.3)	19 (24.0)	

Abbreviations: ALB, serum albumin; ALBI, albumin-bilirubin; ALT, alanine aminotransferase; AST, aspartate aminotransferase; BCLC, Barcelona Clinic Liver Cancer; ECOG-PS, Eastern Cooperative Oncology Group performance status; GGT, Glutamyl transpeptidase; HBV, hepatitis B virus; INR, international normalized ratio; PLT, platelet count; PT, prothrombin time; sCr, serum creatinine; SD, standard deviation; and TBIL, total bilirubin.

Construction and validation of models

A clinical-radiomics model (CR model) was established by combining the radiomics signatures and clinical risk factors. In order to make it more intuitive, the model was presented as a nomogram. In terms of discrimination, calibration, and clinical applicability, the clinical model, radiomics signatures, and CR model were evaluated. The areas under the curves (AUC) of the receiver operating characteristic curves (ROC) from 1 to 3 years were used to assess the discrimination of the model at the different time points [26]. Using the calibration curve to assess the the calibration of the model, the clinical applicability of the model was evaluated by the decision curve [27]. Furthermore, Kaplan-Meier analysis was used to evaluate the OS of the patients and the log-rank test was tested.

To further assess the value of the CR model, using the time-dependent receiver operating characteristic curve to measure the prognostic potential of the CR model versus other clinically validated staging systems, including AJCC TNM systems (eighth edition), Hong Kong Liver Cancer (HKLC stage), China Liver Cancer Staging (CNLC stage), and Japanese integrated score (JIS stage).The patients were analyzed according to BCLC stage (0, A, B, or C) in the prespecified subgroup analysis, tumor diameter (≤5 cm or >5 cm), cirrhosis (absent or present), HBV infection (absent or present), ALBI grade (1, 2, or 3), and Child-Pugh (A or B).

Statistical analyses

The categorical variables were expressed as percentages and analyzed using the Chi-square test or Fisher exact test. The continuous variables were expressed as mean ± standard deviation (SD) or median (range) and analyzed using the Student's *t*-test or Wilcoxon rank sum test. $P < 0.05$ was considered statistically significant in all the hypothesis tests. Open source R software is used to perform statistical analysis and build models. The R packages used in this study include: glmnet, rms, DynNom, plotly, stargazer, nricens, survIDINRI, dcurves, foreign, survival, dplyr, tidyr, timeROC, Hmisc, survminer, stringr, ggcorrplot, ggbump, pROC, survivalROC, ggrisk, and pec.

Results

Study population

A total of 267 patients were included in this study and randomly divided into the training (N = 188) and validation (N = 79) cohorts (Fig. 2). The clinical and radiological characteristics of the patients are listed in Table 1. There were no statistical differences in the characteristics of the patients between the training and validation cohorts (P >0.05). The median follow-up time of the training and validation cohorts was 33.20 and 31.00 months, respectively. A total of 86 (45.74%) and 37 (46.84%) patients died in the training and validation cohorts, respectively.

Radiomics signature

A total of 1316 radiomics features were extracted from each ROI, followed by ICC, Spearman's correlation, and LASSO regression analyses for the selection of features. Among the radiomics signatures in each phase and their combination, the double-phase signature (AP-Signature) showed the best prediction potential (training cohort 1–3 years AUC: 0.729–0.803; validation cohort 1–3 years AUC: 0.750–0.818) (Table 2). The comparison of tumoral and peritumoral radiomics signatures suggested that the signature with tumor and peritumor (5 mm) ROI (AP-TP5-Signature) showed the best performance (Table 2) (training cohort

Table 2
Performances of the different radiomics signatures in the training and validation cohorts.

Radiomics signatures	Training cohort($N = 188$)					Validation cohort($N = 79$)				
	1 year-AUC	2 year-AUC	3 year-AUC	C-index	BS	1 year-AUC	2 year-AUC	3 year-AUC	C-index	BS
A-T	0.697	0.755	0.747	0.670	0.180	0.675	0.756	0.685	0.658	0.197
P-T	0.691	0.748	0.742	0.669	0.182	0.749	0.811	0.724	0.725	0.191
AP-T	0.729	0.803	0.773	0.692	0.169	0.754	0.818	0.750	0.714	0.198
AP-P3	0.702	0.762	0.754	0.673	0.178	0.749	0.785	0.712	0.701	0.195
AP-P5	0.702	0.759	0.753	0.671	0.182	0.628	0.734	0.663	0.626	0.191
AP-TP3	0.746	0.790	0.782	0.699	0.167	0.780	0.774	0.730	0.716	0.206
AP-TP5	0.774	0.846	0.837	0.722	0.151	0.754	0.810	0.772	0.720	0.183

Abbreviations: C-index, the concordance index; BS, the Brier score; A, arterial phase image; P, portal phase image; AP, arterial and portal phase image; AUC, area under the receiver operating characteristic curve; T, tumor region; P3, the peritumor (3 mm) region; P5, the peritumor (5 mm) region; TP3, tumor, and peritumor (3 mm) region; TP5, tumor, and peritumor (5 mm) region.

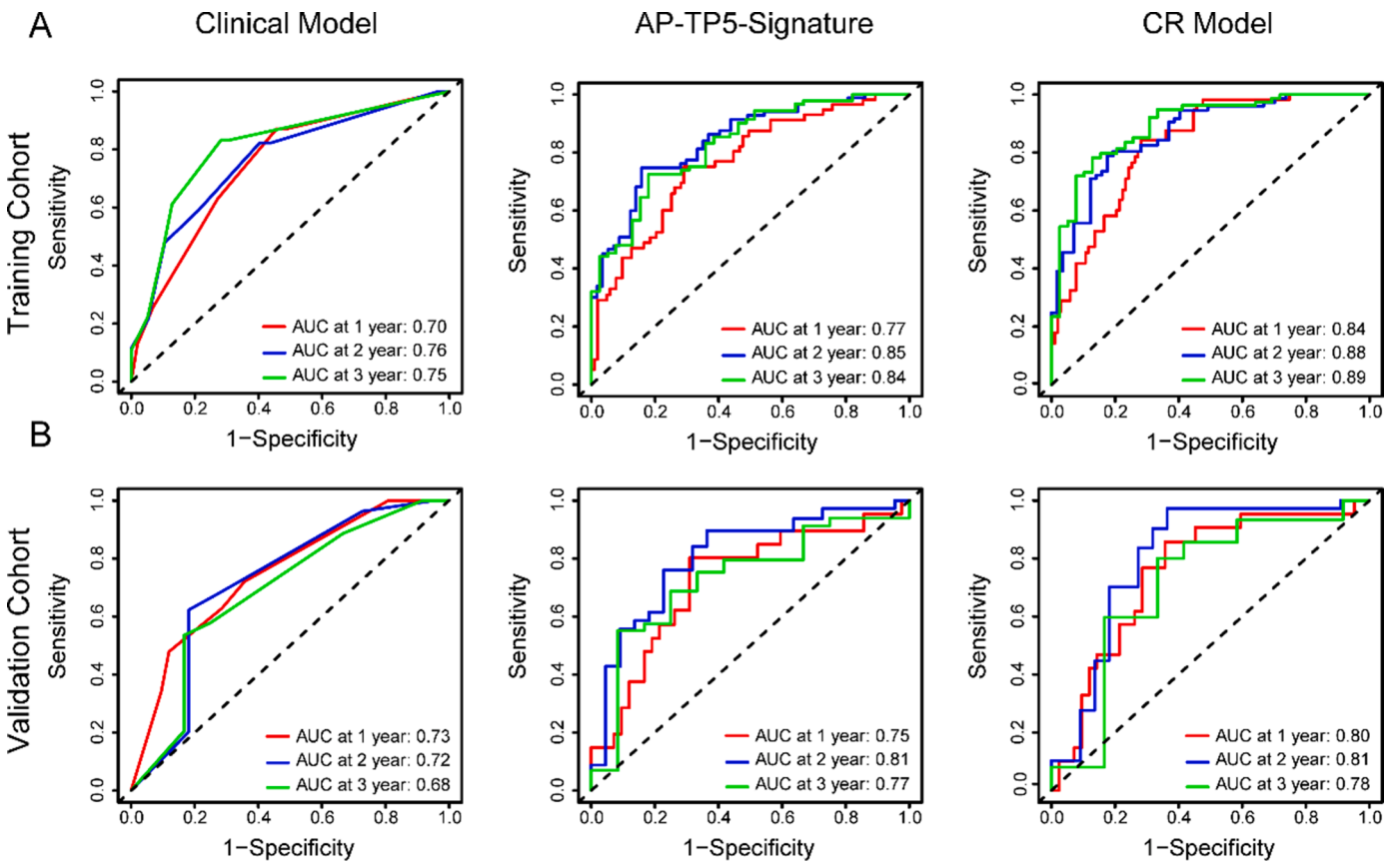

Fig. 3. Time-ROC curves of the clinical model, AP-TP5-Signature, and CR model AUC, areas under the receiver operating characteristic curves; AP-TP5-Signature, the signature with tumor and peritumor (5 mm) ROI; CR, clinical radiomics.

1–3 years AUC: 0.774–0.837; validation cohort 1–3 years AUC: 0.754–0.810) (Table 2). And the AP-TP5 demonstrated a better performance in terms of the concordance index (C-index) and the Brier score (BS) (Table 2). In addition, the AP-TP5-Signature included nine features, three of which were extracted from the tumor ROI and six from the peritumor (5 mm) ROI (Supplementary Table 2).

Clinical variables and radiological characteristics

The univariate analysis resulted in the identification of 10 factors (GGT, ALB, ALBI grade, BCLC stage, cirrhosis, tumor number, tumor location, fusion lesions, intra-tumoral necrosis, tumor diameter), which were significantly correlated with prognosis ($P < 0.05$) (Supplementary Table 3). Multifactorial analysis confirmed that the BCLC stage (HR = 1.49; 95% CI: 1.04–2.12; $P = 0.03$) and cirrhosis (HR = 2.40; 95% CI: 1.46–3.93; $P < 0.001$) were the independent predictors of OS (Supplementary Table 3). Therefore, the clinical models were constructed based on the BCLC stage and cirrhosis using Cox's proportional hazards regression analysis.

Construction and validation of models

Fig. 3 shows the time-dependent ROC (time-ROC) curves of the models. The CR model showed the best discrimination in both the training and validation cohorts (training cohort 1–3 years AUC: 0.837–0.894; validation cohort 1–3 years AUC: 0.781–0.812) as compared to the AP-TP5-Signature and clinical models. Fig. 4 shows the calibration curves of the three models, demonstrating a good agreement between the predicted results of the CR model and actual observed results. Fig. 5 shows the decision curves of the CR model, AP-TP5-Signature, and clinical models. The CR model showed a larger net benefit across the range of reasonable threshold probabilities. The CR

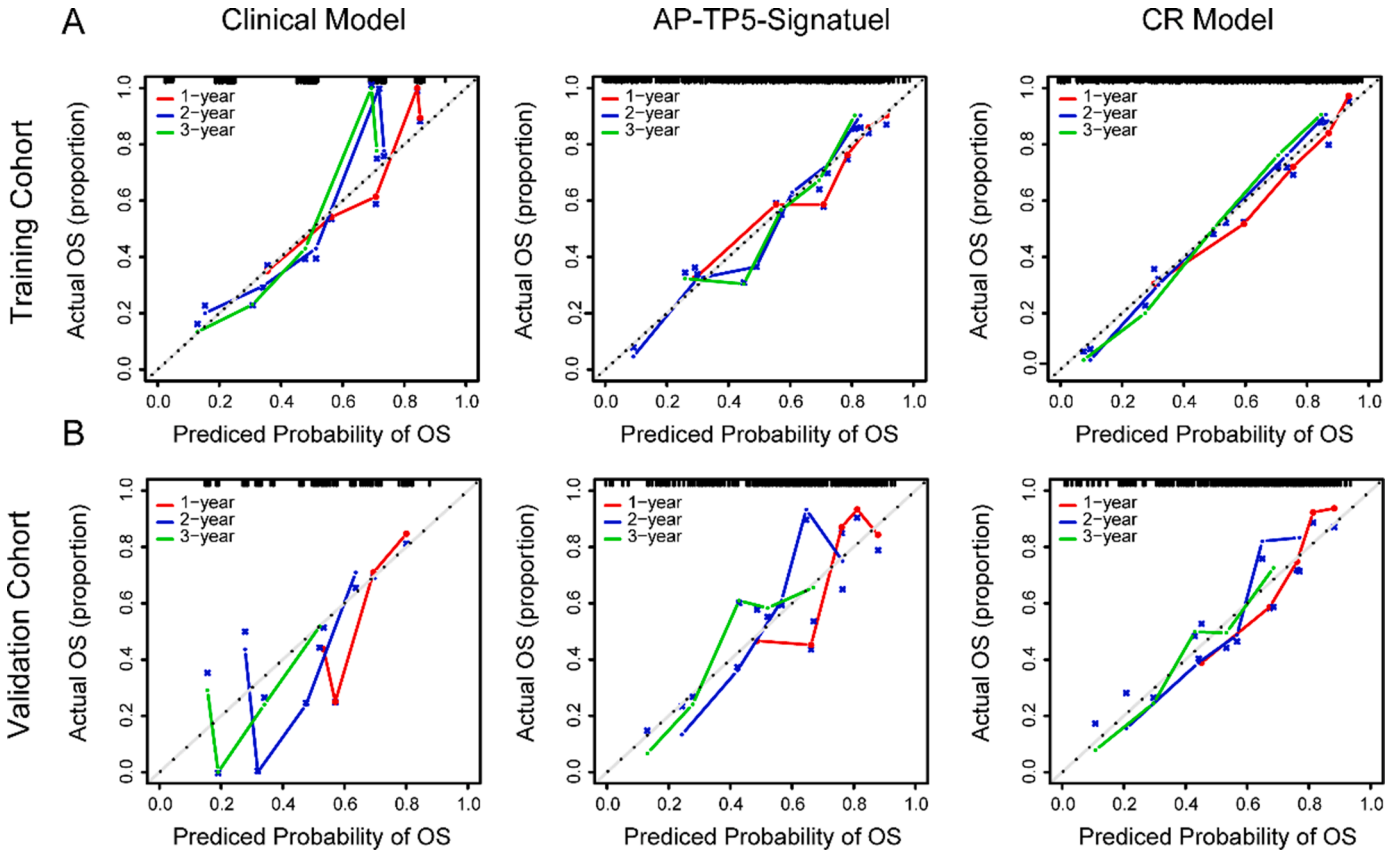

Fig. 4. Calibration curves of the Clinical model, AP-TP5-Signature, and CR model. OS, overall survival; AP-TP5-Signature, the signature with tumor and peritumor (5 mm) ROI; CR, clinical radiomics.

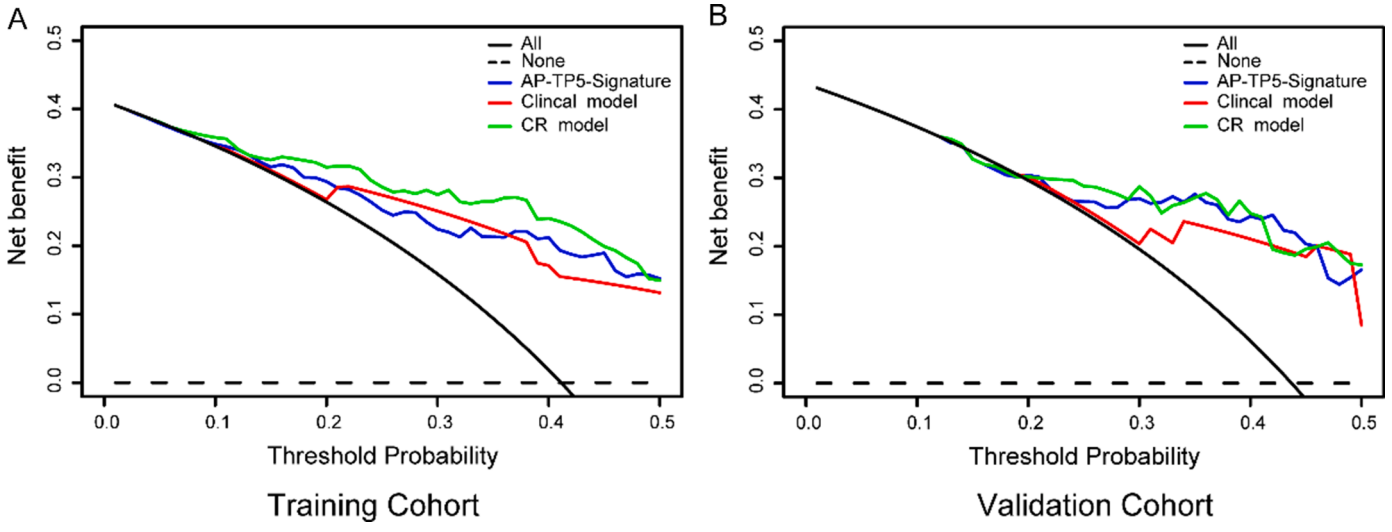

Fig. 5. Decision curves of the Clinical model, AP-TP5-Signature, and CR model. AP-TP5-Signature, the signature with tumor and peritumor (5 mm) ROI; CR, clinical radiomics.

model was visualized using an online calculator of nomogram (Fig. 6).

The time-dependent receiver operating characteristic curve shows that the CR model improved the prediction of HCC survival time compared with other clinically validated staging systems at various time points in both training and validation cohorts (Fig. 7).

The median risk score of the CR model in the training cohort was defined as the cutoff value. The patients were classified into high-risk and low-risk groups. In the training cohort, there was a significant difference in the OS of the patients in the high-risk and low-risk groups (P <0.001; HR = 0.15, 95% CI: 0.09–0.26) (Fig. 8A). This finding was confirmed in the validation cohort (P = 0.018; HR = 0.44, 95% CI: 0.22–0.87) (Fig. 8B). Notably, with the increase in the risk score, the number of cancer-related deaths also increased and that of survivors decreased (Supplementary Figure 1). The characteristics of the CR model are presented in the heatmap (Supplementary Figure 1).

The subgroup analysis showed that the CR model could stratify the

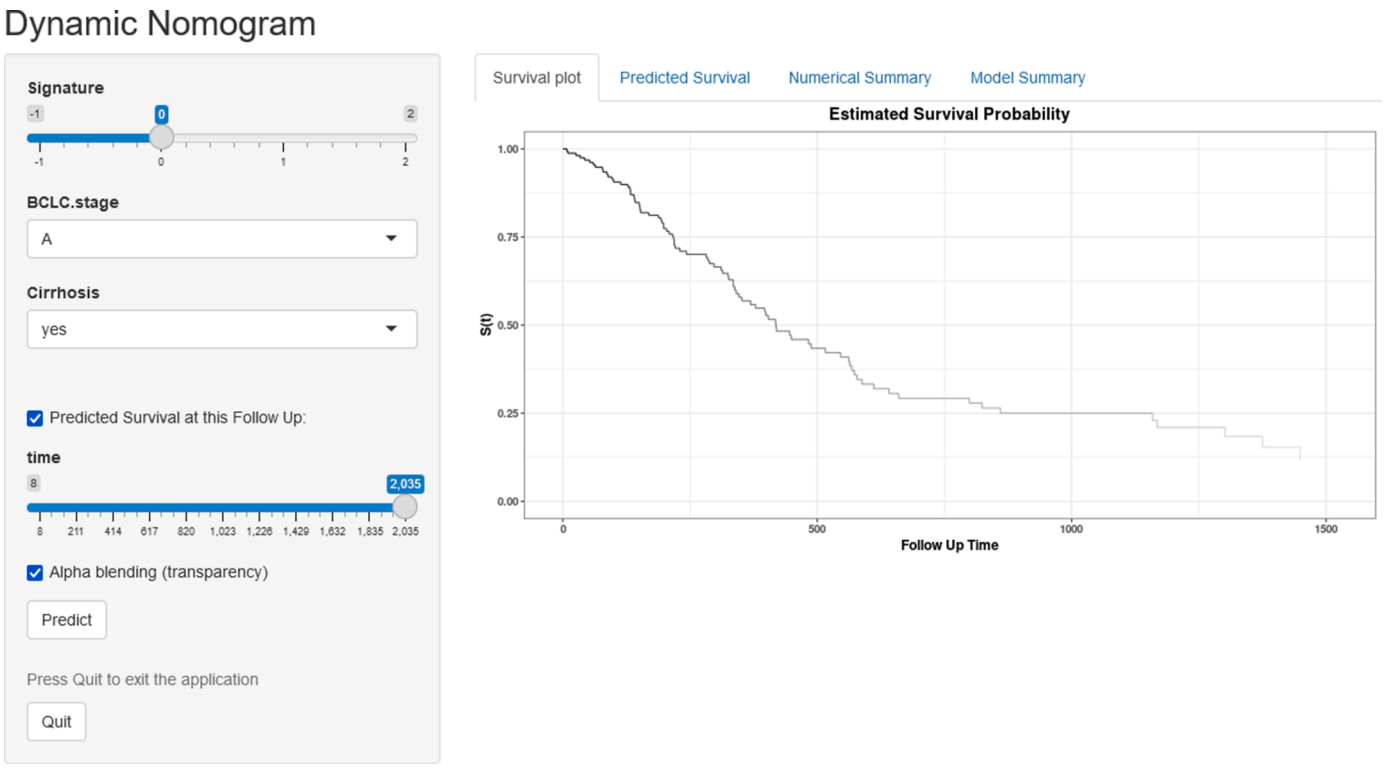

Fig. 6. An online calculator of nomogram based on the CR model, predicting the OS of the patients. The Online tool is available at https://radiomics.shinyapps.io/DynNomapp/. CR, clinical radiomics; OS, overall survival.

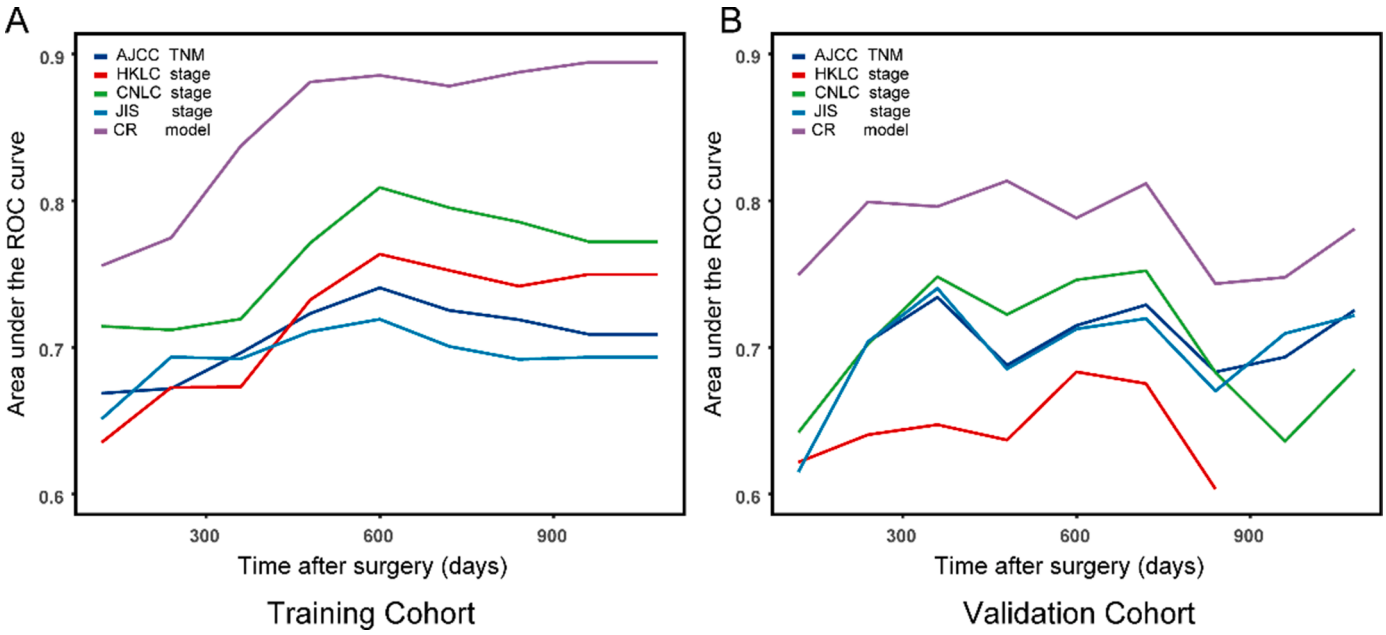

Fig. 7. Discriminatory performance of CR model and systems in training and validation cohorts. Graphs show time-dependent areas under the receiver operating characteristic (ROC) curve at various time points. AJCC, American Joint Committee on Cancer; HKLC, Hong Kong Liver Cancer; CNLC, China Liver Cancer Staging; JIS, Japanese integrated score.

patients in subgroups except ALBI Grade 3, BCLC Stage 0, and BCLC Stage C (Supplementary Figure 2). The subgroup analysis is presented as a forest plot in Supplementary Figure 3.

Discussion

This study established and validated a CR model, which combined the clinical variables (BCLC stage and cirrhosis) and radiomics signatures. As compared to the clinical model, the CR model showed better discrimination, calibration, and clinical applicability. In addition, based on the CR model, the patients could be divided into the high-risk and low-risk groups, having significant differences in their OS.

The analysis of multiphase images is necessary for predicting the prognosis of HCC patients [28]. The multiphase images contain enough

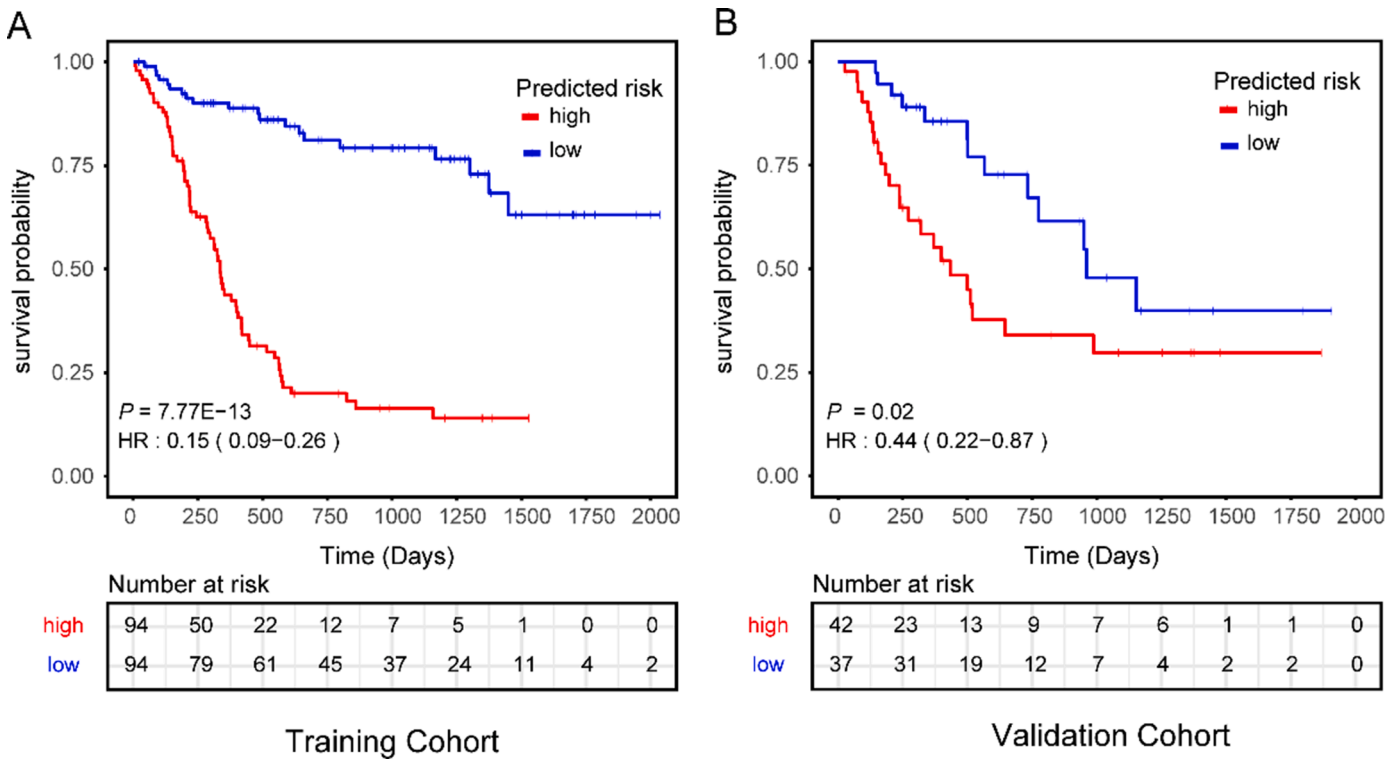

Fig. 8. Kaplan-Meier curves of the OS in the CR model. CR, clinical radiomics; OS, overall survival.

prognostic information to comprehensively reflect the tumor heterogeneity [28,29]. The radiomics features extracted from both the arterial and portal phase images were strongly correlated with the prognosis of the patients with HCC [28,30]. However, previous studies using CT radiomics for predicting the survival of HCC were mainly based on the single-phase images (arterial or portal phase) [16,18]. Therefore, the current study compared the performance of each phase individually as well as in combination. The results confirmed that the double-phase images showed a higher prognostic potential (training cohort AUC:0.729–0.803; validation cohort AUC:0.750–0.818) than their prognostic potential. These results were consistent with the previous prognostic studies [28,31].

There may be potential characteristics in the peritumoral tissue that are important for the prognosis of HCC patients. [15,29]. Recent studies showed that the peritumoral monocytes were associated with tumor invasiveness [32] and peritumoral macrophages could promote venous metastasis [20,21]. The peritumoral stroma enriched in inflammatory cells might provide critical information about micro-metastasis and micro-invasion [19]. On the other hand, several studies confirmed that the radiomics features derived from the peritumoral non-cancerous liver tissues could predict the efficacy and prognosis of transcatheter arterial chemoembolization (TACE) [15,29]. However, most of the previous studies, which predicted the OS of the patients after hepatectomy based on the enhanced CT, did not analyze the peritumoral area [1618]. In this study, the double-phase images of the tumor and peritumor areas were used for the radiomics analysis. The results suggested that the AP-TP5-Signature based on the tumor and peritumor (5 mm) regions, showed better prediction potential (training cohort AUC:0.774–0.846; validation cohort AUC:0.754–0.772). Therefore, the AP-TP5-Signature was selected for further analysis. In addition, the signatures based on tumoral with 5 mm peritumoral area exhibited superior prediction performance. The reason is that the tumoral with 5 mm peritumoral areas may be more appropriate for capturing satellite nodules and microvascular based on the distribution nature of the satellite lesions.

The AP-TP5-Signature consisted of 9 radiomics features, including three shape features, two features of the first order, two features of gray-level co-occurrence matrix (GLCM), and two features of gray-level size zone matrix (GLSZM). The three shape features, including major axis length, maximum 3D diameter, and maximum 2D diameter row, described the tumor size. Studies showed that the tumor size correlated with the tumor malignancy and was an important factor, affecting the prognosis [33]. Among uniformity and the 10th percentile of the first-order features, uniformity was used to measure the consistency of gray-level intensity. A greater uniformity meant lower confounding within the tumor and a better prognosis of the patients. A larger value of the 10th percentile of gray level intensity meant a stronger CT enhancement in the peritumor region, thereby showing worse prognosis potential. This might be due to the occlusion of the portal or hepatic venules due to tumor thrombus, resulting in reduced portal blood flow and compensatory arterial hyper-perfusion [34], which were manifested based on imaging as the peritumoral enhancement and elevated 10th percentile values. The presence of peritumoral enhancement indicated a more aggressive tumor [35,36]. The two features of GLCM included maximum probability (MP) and joint entropy (JE); MP was the maximum probability of the occurrences (neighboring intensive in the predominant pair). A smaller MP value indicated a more complex texture of the peritumoral region. JE was the confusion level of the neighborhood intensity values. A larger JE value indicated a larger non-uniformity in the peritumor region. The GLSZM features included gray-level nonuniformity (GLN) and large area high gray-level emphasis (LAHGLE). GLN was defined as the randomness of the gray-level intensity values. The lower GLN value indicated more homogeneity in the intensity values. LAHGLE was the weight of the large size zones with the high gray-level values. The MP, JE, GLN, and LAHGLE values reflected the different aspects of tumoral and peritumoral heterogeneity. The tumors with greater heterogeneity had a poorer prognosis. Previous studies demonstrated that tumor heterogeneity was an important prognostic factor [37,38] These features can be used to characterize and quantify the tumor genomic heterogeneity by reflecting the tumor necrosis, hemorrhage, and hypoxia and using the information of the spatial distribution of gray-level values. Previous studies supported the inference of proteogenomic and phenotypic information from the analysis of

CT images [39,40].

In terms of discrimination, calibration, and clinical applicability, the CR model showed excellent ability. Therefore, it was suggested that a multivariate model, combining the clinical and radiomics features, was feasible for the prognosis of HCC patients. Furthermore, the CR model could classify the patients into high-risk and low-risk groups, thereby confirming its prognostic potential. Considering the confounding factors of the study population, a prespecified subgroup analysis was performed to explore the prognostic potential of the CR model in the different subgroups. In most subgroups, the CR model could risk-stratify the subgroups. However, the CR model failed to complete the risk stratification in the ALBI Class 3, BCLC Stage 0, and BCLC Stage C subgroups, which might be due to the small sample size of these subgroups. Similarly, the risk stratification had also failed in other studies due to the small sample size [41,42].

There were limitations to this study. First, the patients in this study were recruited from a single cohort. In order to verify the generalizability of the model, these results should be validated in other cohorts. Second, this study used the manual outlining of the ROIs, which was time-consuming and laborious. The subsequent consideration of semi-automated or automated outlining of the ROIs is needed to simplify the work task. Third, this was a retrospective study. Although bias had been minimized, certain clinical factors remained uncontrolled, such as the different treatments given to the patients after hepatectomy. This factor might also affect the OS of the patients. Fourth, the model established in this study was based on Chinese patients only. There are differences in the etiology of Chinese and western patients. In addition, for patients with intermediate and advanced liver cancer, Western physicians and guidelines prefer palliative treatment to control tumor growth, while Asian physicians and guidelines prefer radical treatment. Therefore, the validity of the model would be subsequently verified in Western populations. Fifth, the usefulness of the model was still insufficient. Our model cannot automatically outline the ROI and calculate the radiomics-signature. So, applying the model to the clinic is still difficult.

In conclusion, a model was established for predicting the OS of hepatectomy in the HCC patients, which could assist the clinicians in building a personalized treatment plan for the patients. However, further studies are needed to verify the generalizability of the model and translate these results into clinical practice.

Declaration of Competing Interest

The authors declare that they have no known competing financial interests or personal relationships that could have appeared to influence the work reported in this paper.

Funding information

his work was supported by the Nanchong City-School Science and Technology Strategic Cooperation Project (NSMC20170301) and the Nanchong City-School Science and Technology Strategic Cooperation Project (19SXHZ0239)..

Informed consent

Written informed consent was waived by the Institutional Review Board.

Ethical approval

Institutional Review Board approval was obtained.
Methodology
Retrospective
Diagnostic study
Performed at one institution

Supplementary materials

Supplementary material associated with this article can be found, in the online version, at doi:10.1016/j.tranon.2022.101536.

References

[1] H SUNG, J FERLAY, RL SIEGEL, et al., Global cancer statistics 2020: GLOBOCAN estimates of incidence and mortality worldwide for 36 cancers in 185 countries, CA Cancer J. Clin. (2021).
[2] M GERLINGER, AJ ROWAN, S HORSWELL, et al., Intratumor heterogeneity and branched evolution revealed by multiregion sequencing, N. Engl. J. Med. 366 (10) (2012) 883–892.
[3] A FORNER, M REIG, J BRUIX, Hepatocellular carcinoma, Lancet 391 (10127) (2018) 1301–1314.
[4] B YANG, B ZHENG, M YANG, et al., Liver resection versus transarterial chemoembolization for the initial treatment of barcelona clinic liver cancer stage B hepatocellular carcinoma, Hepatol. Int. 12 (5) (2018) 417–428.
[5] L YIN, H LI, AJ LI, et al., Partial hepatectomy vs. transcatheter arterial chemoembolization for resectable multiple hepatocellular carcinoma beyond milan criteria: a RCT, J. Hepatol. 61 (1) (2014) 82–88.
[6] DI TSILIMIGRAS, F BAGANTE, D MORIS, et al., Recurrence patterns and outcomes after resection of hepatocellular carcinoma within and beyond the barcelona clinic liver cancer criteria, Ann. Surg. Oncol. 27 (7) (2020) 2321–2331.
[7] YN ZHAO, YQ ZHANG, JZ YE, et al., Hepatic resection versus transarterial chemoembolization for patients with Barcelona clinic liver cancer intermediate stage child-pugh A hepatocellular carcinoma, Exp. Ther. Med. 12 (6) (2016) 3813–3819.
[8] I LABGAA, P TAFFé, D MARTIN, et al., Comparison of partial hepatectomy and transarterial chemoembolization in intermediate-stage hepatocellular carcinoma: a systematic review and meta-analysis, Liver Cancer 9 (2) (2020) 138–147.
[9] Y KAWAGUCHI, K HASEGAWA, Y HAGIWARA, et al., Effect of diameter and number of hepatocellular carcinomas on survival after resection, transarterial chemoembolization, and ablation, Am. J. Gastroenterol. 116 (8) (2021) 1698–1708.
[10] M KANDA, H SUGIMOTO, Y KODERA, Genetic and epigenetic aspects of initiation and progression of hepatocellular carcinoma, World J. Gastroenterol. 21 (37) (2015) 10584–10597.
[11] EJ LIMKIN, R SUN, L DERCLE, et al., Promises and challenges for the implementation of computational medical imaging (radiomics) in oncology, Ann. Oncol. 28 (6) (2017) 1191–1206.
[12] P LAMBIN, RTH LEIJENAAR, TM DEIST, et al., Radiomics: the bridge between medical imaging and personalized medicine, Nat. Rev. Clin. Oncol. 14 (12) (2017) 749–762.
[13] GJ WEISS, B GANESHAN, KA MILES, et al., Noninvasive image texture analysis differentiates K-ras mutation from pan-wildtype NSCLC and is prognostic, PLoS One 9 (7) (2014) e100244.
[14] J JIN, Z YAO, T ZHANG, et al., Deep learning radiomics model accurately predicts hepatocellular carcinoma occurrence in chronic hepatitis B patients: a five-year follow-up, Am. J. Cancer Res. 11 (2) (2021) 576–589.
[15] M CHEN, J CAO, J HU, et al., Clinical-radiomic analysis for pretreatment prediction of objective response to first transarterial chemoembolization in hepatocellular carcinoma, Liver Cancer 10 (1) (2021) 38–51.
[16] BH ZHENG, LZ LIU, ZZ ZHANG, et al., Radiomics score: a potential prognostic imaging feature for postoperative survival of solitary HCC patients, BMC Cancer 18 (1) (2018) 1148.
[17] H AKAI, K YASAKA, A KUNIMATSU, et al., Predicting prognosis of resected hepatocellular carcinoma by radiomics analysis with random survival forest, Diagn. Interv. Imaging 99 (10) (2018) 643–651.
[18] Q LIU, J LI, F LIU, et al., A radiomics nomogram for the prediction of overall survival in patients with hepatocellular carcinoma after hepatectomy, Cancer Imaging 20 (1) (2020) 82.
[19] DM KUANG, C PENG, Q ZHAO, et al., Activated monocytes in peritumoral stroma of hepatocellular carcinoma promote expansion of memory T helper 17 cells, Hepatology 51 (1) (2010) 154–164.
[20] A MANTOVANI, S SOZZANI, M LOCATI, et al., Macrophage polarization: tumor-associated macrophages as a paradigm for polarized M2 mononuclear phagocytes, Trends Immunol. 23 (11) (2002) 549–555.
[21] A BUDHU, M FORGUES, QH YE, et al., Prediction of venous metastases, recurrence, and prognosis in hepatocellular carcinoma based on a unique immune response signature of the liver microenvironment, Cancer Cell 10 (2) (2006) 99–111.
[22] R ZHANG, L XU, X WEN, et al., A nomogram based on bi-regional radiomics features from multimodal magnetic resonance imaging for preoperative prediction of microvascular invasion in hepatocellular carcinoma, Quant Imaging Med. Surg. 9 (9) (2019) 1503–1515.
[23] XM DAI, T HUANG, SL YANG, et al., Peritumoral EpCAM is an independent prognostic marker after curative resection of HBV-related hepatocellular carcinoma, Dis. Markers (2017), 2017 8495326.
[24] LQ KONG, XD ZHU, HX XU, et al., The clinical significance of the CD163+ and CD68+ macrophages in patients with hepatocellular carcinoma, PLoS One 8 (3) (2013) e59771.

[25] JJM VAN GRIETHUYSEN, A FEDOROV, C PARMAR, et al., Computational radiomics system to decode the radiographic phenotype, Cancer Res. 77 (21) (2017) e104-e7.
[26] PJ HEAGERTY, T LUMLEY, MS PEPE, Time-dependent ROC curves for censored survival data and a diagnostic marker, Biometrics 56 (2) (2000) 337–344.
[27] A VICKERS, ELKINEB J, Decision curve analysis: a novel method for evaluating prediction models, Med. Decis. Making 26 (6) (2006) 565–574.
[28] S KIM, J SHIN, DY KIM, et al., Radiomics on Gadoxetic Acid-enhanced magnetic resonance imaging for prediction of postoperative early and late recurrence of single hepatocellular carcinoma, Clin. Cancer Res. 25 (13) (2019) 3847–3855.
[29] XP MENG, YC WANG, S JU, et al., Radiomics Analysis on multiphase contrast-enhanced CT: a survival prediction tool in patients with hepatocellular carcinoma undergoing transarterial chemoembolization, Front. Oncol. 10 (2020) 1196.
[30] DB HASDEMIR, LA DáVILA, N SCHWEITZER, et al., Evaluation of CT vascularization patterns for survival prognosis in patients with hepatocellular carcinoma treated by conventional TACE, Diagn Interv Radiol 23 (3) (2017) 217–222.
[31] Y ZHAO, J WU, Q ZHANG, et al., Radiomics analysis based on multiparametric mri for predicting early recurrence in hepatocellular carcinoma after partial hepatectomy, J. Magn. Reson. Imaging 53 (4) (2021) 1066–1079.
[32] DP CHEN, WR NING, XF LI, et al., Peritumoral monocytes induce cancer cell autophagy to facilitate the progression of human hepatocellular carcinoma, Autophagy 14 (8) (2018) 1335–1346.
[33] F LIANG, F MA, J ZHONG, Prognostic factors of patients after liver cancer surgery: based on Surveillance, Epidemiology, and End Results database, Medicine 100 (30) (2021) e26694.
[34] O MATSUI, S KOBAYASHI, J SANADA, et al., Hepatocelluar nodules in liver cirrhosis: hemodynamic evaluation (angiography-assisted CT) with special reference to multi-step hepatocarcinogenesis, Abdom. Imaging 36 (3) (2011) 264–272.
[35] M RENZULLI, S BROCCHI, A CUCCHETTI, et al., Can current preoperative imaging be used to detect microvascular invasion of hepatocellular carcinoma? Radiology 279 (2) (2016) 432–442.
[36] A NISHIE, K YOSHIMITSU, Y ASAYAMA, et al., Radiologic detectability of minute portal venous invasion in hepatocellular carcinoma, AJR Am. J. Roentgenol. 190 (1) (2008) 81–87.
[37] S BONIN, G STANTA, Pre-analytics and tumor heterogeneity, N Biotechnol. 55 (2020), 30-5.
[38] Y YUAN, Spatial Heterogeneity in the Tumor Microenvironment, Cold Spring Harb. Perspect. Med. 6 (8) (2016).
[39] AM RUTMAN, MD KUO, Radiogenomics: creating a link between molecular diagnostics and diagnostic imaging, Eur. J. Radiol. 70 (2) (2009) 232–241.
[40] P GROSSMANN, O STRINGFIELD, N EL-HACHEM, et al., Defining the biological basis of radiomic phenotypes in lung cancer, Elife 6 (2017).
[41] JX ZHANG, W SONG, ZH CHEN, et al., Prognostic and predictive value of a microRNA signature in stage II colon cancer: a microRNA expression analysis, Lancet Oncol. 14 (13) (2013) 1295–1306.
[42] Y HUANG, Z LIU, L HE, et al., Radiomics signature: a potential biomarker for the prediction of disease-free survival in early-stage (i or ii) non-small cell lung cancer, Radiology 281 (3) (2016) 947–957.